Anal Bioanal Chem (2013) 405:2545–2552
DOI 10.1007/s00216-012-6634-y

ORIGINAL PAPER

Development of a stable biosensor based on a SiO_2 nanosheet–Nafion–modified glassy carbon electrode for sensitive detection of pesticides

Long Yang · Guang-Can Wang · Yong-Jun Liu · Jing-Jing An · Min Wang

Received: 17 September 2012 / Revised: 25 November 2012 / Accepted: 6 December 2012 / Published online: 27 January 2013

Abstract SiO_2 nanosheets (SNS) have been prepared by a chemical method using montmorillonite as raw material and were characterized by scanning electron microscopy and X-ray diffraction. SiO_2 nanosheet–Nafion nanocomposites with excellent conductivity, catalytic activity, and biocompatibility provided an extremely hydrophilic surface for biomolecule adhesion. Chitosan was used as a cross-linker to immobilize acetylcholinesterase (AChE), and Nafion was used as a protective membrane to efficiently improve the stability of the AChE biosensor. The AChE biosensor showed favorable affinity for acetylthiocholine chloride and catalyzed the hydrolysis of acetylthiocholine chloride with an apparent Michaelis–Menten constant of 134 μM to form thiocholine, which was then oxidized to produce a detectable and fast response. Based on the inhibition by pesticides of the enzymatic activity of AChE, detection of the amperometric response from thiocholine on the biosensor is a simple and effective way to biomonitor exposure to pesticides. Under optimum conditions, the biosensor detected methyl parathion, chlorpyrifos, and carbofuran at concentrations ranging from 1.0×10^{-12} to 1×10^{-10}M and from 1.0×10^{-10} to 1×10^{-8}M. The detection limits for methyl parathion, chlorpyrifos, and carbofuran were 5×10^{-13}M. The biosensor developed exhibited good sensitivity, stability, reproducibility, and low cost, thus providing a new promising tool for analysis of enzyme inhibitors.

Keywords SiO_2 nanosheets · Acetylcholinesterase · Chitosan · Nafion · Amperometric biosensor

Introduction

Pesticides have played an important role in increasing agricultural productivity. Owing to their bioaccumulation effect, they can cause long-term damage to both the environment and health even though their concentration is very low [1, 2]. Pesticides may have negative effects on the visual system, sensory function, cognitive function, and nervous system which result in severe health problems in both animals and humans. Therefore, the quantitative detection of organophosphate pesticides is quite significant. In recent years, biosensors based on acetylcholinesterase (AChE) have emerged as a promising technique for toxicity analysis, environmental monitoring, food quality control, and military investigations [3–5]. The main application of AChE biosensors is for the detection of organophosphate and carbamate pesticides based on enzyme inhibition. These devices are designed to complement or replace existing reference analytical methods (high-performance liquid chromatography and gas chromatography/mass spectrometry) by simplifying or eliminating sample preparation, thus decreasing the analysis time and cost.

The nano-silica materials discovered by scientists at Mobil in 1992 were quickly recognized as a breakthrough that could lead to a variety of important applications [6]. SiO_2 nanosheets (SNS) are a class of important catalysts and adsorbents which allow fast transport of bulky molecules and thereby result in improved performance in petrochemical and biomass processing [7]. Consequently, the large surface area of these materials (700–1,500 m^2g^{-1}), along with the biocompatibility, nontoxicity, high ionic conductivity, and chemical and thermal stability of silicon, makes

Electronic supplementary material The online version of this article (doi:10.1007/s00216-012-6634-y) contains supplementary material, which is available to authorized users.

L. Yang · G.-C. Wang (✉) · Y.-J. Liu · J.-J. An · M. Wang
School of Chemical Science and Engineering, Yunnan University, Kunming 650091, China
e-mail: wangc166163@sina.com

them ideal for use as supports for adsorption, catalysis, chemical separations, biosensors, etc. [8–11]. Therefore, there is a considerable scope to explore the properties of SNS for application to biosensors.

Nafion (NF) is a perfluorosulfonate cation-exchange resin that is chemically and thermally inert, nonelectroactive, hydrophilic, and insoluble in water, thus possessing almost ideal properties for preparation of modified electrodes [12, 13]. Together with some nanomaterials with high conductivity and catalytic activity, use of NF seems to be a possible approach to improve the sensitivity and selectivity of modified electrodes. Sensors formed from NF and nanomaterials not only exhibit strong catalytic activity but also exhibit good stability and reproducibility [14–17].

We prepared SNS by a chemical method using montmorillonite as raw material. The inorganic and organic compounds contained in montmorillonite were eliminated after the montmorillonite with a sandwich structure of SNS and inorganic and organic compounds had been treated with nitric acid, hydrochloric acid, and perchloric acid. The SNS showed excellent properties such as high conductivity, catalytic activity, strong adsorptivity, and low cost. Currently, the stability of the biosensor is one of the key challenges in the development of biosensors based on AChE inhibition. In this work, to improve the stability of the biosensor, chitosan (CS) was used as a cross-linker to immobilize AChE on an SNS–NF modified glassy carbon electrode (GCE) and NF was used as a protective membrane in the AChE biosensors to improve the stability of the biosensor.

In this work, combining the excellent properties of SNS, CS, and NF, we used the nanocomposites to structure an extremely hydrophilic surface for biomolecule adhesion, and obtained a sensitive and stable AChE biosensor. Owing to the high conductivity and catalytic activity of the nanocomposites, the biosensor showed favorable affinity for acetylthiocholine chloride (ATCl) and catalyzed the hydrolysis of ATCl at a low applied potential with high sensitivity, fast response, acceptable stability, reproducibility, low cost, and convenient preparation. It might be an effective candidate for analysis of other enzyme inhibitors.

Experimental

Reagents and apparatus

ATCl, AChE (type C3389, 500 U mg^{-1} from electric eel), NF (5 % in lower aliphatic alcohols and water), CS, and pyridine 2-aldoxime methiodide (PAM) were purchased from Sigma-Aldrich (St. Louis, USA). Methyl parathion, chlorpyrifos, and carbofuran (purity 99.99 % or greater) were obtained from the Institute of Environmental Protection of China's Agriculture Ministry (Beijing, China). The montmorillonite was purchased from Beaufour Ipsen Pharmaceutical (Tianjin, China). All other chemicals and reagents were of analytical grade. Aqueous solutions were prepared with deionized water.

The electrochemical measurements were performed with an IM6ex electrochemical workstation (Zahne Elektrik Instruments, Germany). A conventional three-electrode system was employed with a saturated calomel electrode as the reference electrode, a platinum foil as the counter electrode, and the modified GCEs (diameter 3 mm) as the working electrode. Amperometric measurements were performed in 0.1 M phosphate-buffered saline (PBS; pH 7.4) by cyclic voltammetry (CV). All experiments were performed at room temperature (25±1 °C). SNS were characterized by scanning electron microscopy (Quanta 50 scanning electron microscope, FEI, USA) and X-ray diffraction (TTRIII X-ray diffractometer, Rigaku, Japan).

Preparation of SNS

SNS were prepared using montmorillonite as raw material. Briefly, 3.0 g of montmorillonite was dissolved in 5.0 ml of deionized water, and then 20 ml of nitric acid, 20 ml of hydrochloric acid, and 5.0 ml of perchloric acid were added to the montmorillonite aqueous solution. Then, the mixture was heated to 150 °C on an electric hot plate for 5 h. When it had almost dried, the solution was added to 10 ml of hydrochloric acid. The resulting mixture was headed for 10 min and the white suspension that formed was separated by centrifugation at 12,000 rpm, washed with deionized water several times, and dried in an oven at 50 °C to obtain SNS.

Preparation of SNS–NF nanocomposites

NF solution (0.125 %, w/v) was prepared by diluting 5 % NF with ethanol and deionized water (1:1, v/v). The SNS (0.5 mg) were added to 1.0 ml of NF solution and the mixture was sonicated thoroughly until a homogeneous suspension was obtained. The suspensions were stored under refrigeration (4 °C) when not in use.

Preparation of the AChE biosensor

A GCE was polished carefully to a mirror-like finish with 0.3- and 0.05-μm alumina slurry and sequentially sonicated for 3 min in nitric acid (9M), ethanol, and water. Before the experiment, a potential of +1.75 V was applied to the electrode under stirring in pH 5.0 PBS for 300 s, and then the electrode was electrochemically pretreated by cycling the potential repeatedly between +0.3 and +1.25 V and between +0.3 and −1.3 V until a steady-state current–voltage curve was obtained. The SNS–NF/GCE was obtained

by casting 5 μl SNS-NF suspension onto the GCE in the same way as the NF/GCE was obtained and was dried at room temperature. The AChE–CS solution contained 0.05 U AChE and 0.2 % CS (w/v, 50 mM acetic acid). The electrodes obtained were finally coated with 4.5 μl AChE–CS (2:1, v/v) solutions. The modified electrodes were washed with pH 7.4 PBS to remove the unbound AChE. AChE–CS/GCE, AChE–CS/NF/GCE, and AChE–CS/SNS–NF/GCE biosensors were obtained. The biosensors were covered with 3 μl of 0.1 % (w/v) NF as a protective membrane and stored at 4 °C when not in use.

Detection of the ATCl

The typical current–time plot for the biosensor was obtained at 0.65 V after the successive addition of ATCl to PBS with stirring. The apparent Michaelis–Menten constant K_m^{app} of the biosensor was calculated from the Lineweaver–Burk equation [18]:

$$\frac{1}{i_{ss}} = \left(\frac{K_m^{app}}{i_{max}}\right)\left(\frac{1}{C}\right) + \left(\frac{1}{i_{max}}\right), \quad (1)$$

where i_{ss} is the steady-state current after the addition of substrate, i_{max} is the maximum current measured under the condition of saturated substrate, and C is the concentration of the substrate. The K_m^{app} value, which gives an indication of the enzyme–substrate kinetics for the biosensor, was determined by analysis of the slope and intercept of the plot of the reciprocal of the steady-state current versus ATCl concentration.

Detection of the pesticides

The NF/AChE–CS/SNS–NF/GCE obtained was first immersed in pH 7.4 PBS containing different concentrations of standard pesticide at room temperature (25±1 °C) for 6 min and was then transferred to an electrochemical cell of pH 7.4 PBS containing 0.5 mM ATCl to study the amperometric response by CV between 0.0 and 1.0 V. The inhibition caused by the pesticide was calculated as follows:

$$\text{Inhibition } (\%) = \frac{i_{p,control} - i_{p,exp}}{i_{p,control}} \times 100\%, \quad (2)$$

where $i_{p,control}$ is the peak current of ATCl on the NF/AChE–CS/SNS–NF/GCE and $i_{p,exp}$ is the amperometric response of ATCl on the NF/AChE–CS/SNS–NF/GCE with pesticide inhibition.

Regeneration of AChE

After the pesticides had been tested, the AChE biosensor was rinsed with 0.1 M PBS, and was then incubated in 0.1 M PBS containing 0.1 mM PAM and 0.1 M PBS containing 10 mM ATCl, respectively, for 2 min. Moreover, the AChE biosensor was used for the next determination. The successive rinsing and incubation in 0.1 mM PAM and 10 mM ATCl, respectively, were used to regenerate the biosensor.

Preparation and determination of real samples

Apple and cabbage samples were obtained from a local market in Kunming City. Briefly, the apple and cabbage were cleaned and mashed to pulp with a blender, and then two sorts of 25.0 g pulp were mixed with 50 ml acetonitrile and an appropriate amount of 0.1 M NaCl, respectively. The organic phases were collected and evaporated on a steam bath. The final volume was adjusted to 5.0 ml by adding an appropriate amount of dichloromethane. Part of the sample solution was transferred to 0.01 M PBS (pH 7.4) for determination.

Results and discussion

Characterization of SNS

The scanning electron microscope image of SNS (Fig. 1) revealed that the SNS consisted of random aggregates of thin sheets with thickness of about 10 nm. X-ray diffraction of SNS (Fig. 2) exhibited a major reflection plane at 2θ= 21.85° corresponding to the (0 0 2) reflection plane and is consistent with the standard pattern for orthorhombic SiO_2 (JSPDS 00-050-1432).

Electrochemical behavior of the NF/AChE–CS/SNS–NF/GCE

The CV of ATCl and the enzymatic product thiocholine was investigated on the NF/AChE–CS/GCE, NF/AChE–CS/NF/GCE, and NF/AChE–CS/SNS–NF/GCE, respectively, as

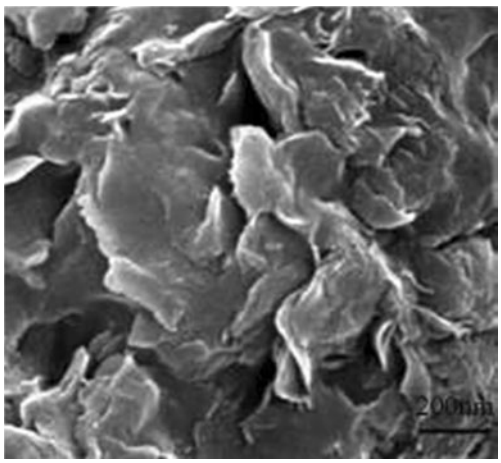

Fig. 1 Scanning electron microscope image of SiO_2 nanosheets (SNS)

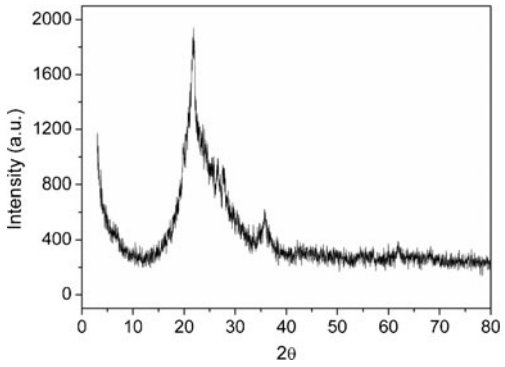

Fig. 2 X-ray diffraction image of SNS

shown in Fig. 3. No amperometric response was observed at the NF/AChE–CS/GCE, NF/AChE–CS/NF/GCE, and NF/AChE–CS/SNS–NF/GCE in pH 7.4 PBS (Fig. 3). However, when 0.5 mM ATCl was added to pH 7.4 PBS, obvious amperometric responses were observed at the NF/AChE–CS/GCE, NF/AChE–CS/NF/GCE, and NF/AChE–CS/SNS–NF/GCE (Fig. 3). Obviously, these amperometric responses were attributed to the oxidation of thiocholine, the hydrolysis product of ATCl, which was catalyzed by immobilized AChE. Figure 3 shows the oxidation peak currents increased orderly, and the oxidation peak potentials shifted negatively orderly. The oxidation peak current at the NF/AChE–CS/SNS–NF/GCE (Fig. 3, curve f) is much higher and the oxidation peak potential is lower than those of the other electrodes. Thus, these results indicate that NF and SNS–NF improved the conductivity and catalytic activity. The decrease of the overpotential of thiocholine oxidation is beneficial for avoiding interference from other electroactive species in biological mixtures.

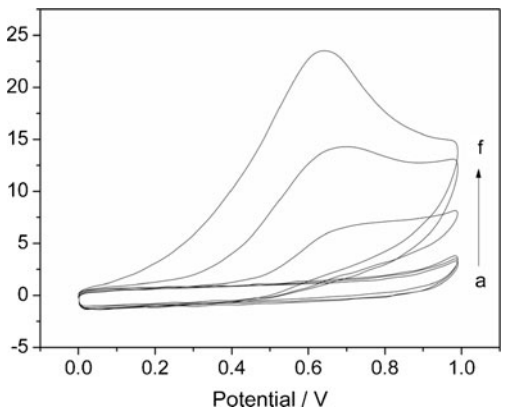

Fig. 3 Cyclic voltammograms in order from *a* to *f* of the Nafion (NF)/acetylcholinesterase (AChE)–chitosan (CS)/glassy carbon electrode (GCE), NF/AChE–CS/NF/GCE, and NF/AChE–CS/SNS–NF/GCE in 0.1 M phosphate-buffered saline (PBS) and the NF/AChE–CS/GCE, NF/AChE–CS/NF/GCE, and NF/AChE–CS/SNS–NF/GCE in 0.1 M PBS containing 0.5 mM acetylthiocholine chloride (ATCl). Scan rate 0.10 Vs^{-1} at 25 °C

Optimization of the preparation of the biosensor

The effect of SNS content on the amperometric response was studied from 0.1 to 0.9 $mg\,ml^{-1}$ (modified amount 5 μl). The amperometric response gradually increased with increasing SNS content and reached a maximum at 0.5 mg ml^{-1}. Further increasing the content of SNS led to a gradual decrease of the amperometric response, possibly because of increased resistance and double-layer capacitance of the modified electrode. As a result of these experiments, 0.5 $mg\,ml^{-1}$ SNS was used for preparation of the biosensor.

The amperometric response was also affected by the content of NF in the NF–SNS suspension. When the content of NF changed from 0.075 % to 0.150 % (w/v), the amperometric response gradually increased with increasing NF content and reached a maximum at 0.125 % (w/v). Further increase of the amount of NF led to a gradual decrease of the amperometric response. Possibly, the lower NF content was disadvantageous for formation of the SNS–NF film and reduced the catalytic activity and conductivity. Nevertheless, the higher NF content increased the resistance and reduced the catalytic activity of SNS–NF. Therefore, 0.125 % (w/v) NF was used for preparation of the SNS–NF suspension.

The amount of AChE immobilized on the electrode surface was another important aspect of the preparation of the AChE biosensor. As the amount of AChE changed from 0.10 to 0.20 U, the amperometric response of the biosensor increased and reached a maximum at 0.15 U. Further increase of the amount of AChE led to a gradual decrease of the amperometric response. Possibly the lesser amount of AChE was not enough to catalyze hydrolysis of ATCl. Furthermore, superabundant AChE possibly increased resistance of the modified electrode and it was not stable enough. Thus, 0.15 U of AChE was used in these experiments.

To enhance the stability of the biosensor, CS was used as a cross-linker to immobilize the AChE on the SNS–NF/GCE and improve conductivity between AChE and the SNS–NF/GCE. Furthermore, the surface of the biosensor was covered with 3 μl of 0.1 % (w/v) NF as a protective membrane. For comparison, the relative standard deviations (RSDs) of the amperometric responses of the AChE/SNS–NF/GCE, AChE–CS/SNS–NF/GCE, and NF/AChE–CS/SNS–NF/GCE biosensors were continuously tested six times, respectively, in pH 7.4 PBS containing 0.5 mM ATCl (Fig. 4). The RSD (11.5 %, Fig. 4, curve b, standard deviation 2.347) of the amperometric response of the AChE–CS/SNS–NF/GCE biosensor was less than the RSD (18.2 %, Fig. 4, curve c, standard deviation 4.043) of the amperometric response of the AChE/SNS–NF/GCE biosensor. The RSD (3.4 %, Fig. 4, curve a, standard deviation 0.597) of the amperometric response of the NF/AChE–CS/SNS–NF/GCE biosensor was the least of the three biosensors. The

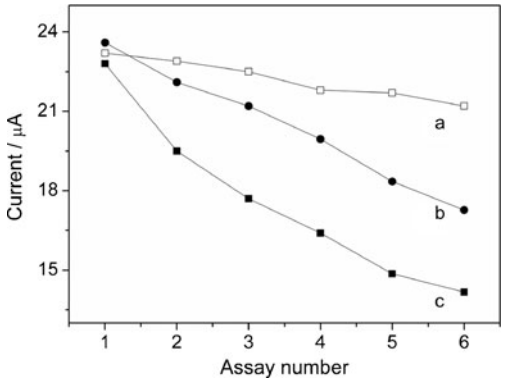

Fig. 4 The relative standard deviation of the amperometric response of the NF/AChE–CS/SNS–NF/GCE (**a**), AChE–CS/SNS–NF/GCE (**b**), and AChE/SNS–NF/GCE (**c**)

results showed that CS as a cross-linker immobilized AChE and the NF protective membrane effectively improved the stability of the AChE biosensor.

That the amperometric response and the RSD of the amperometric response were affected by the amount of NF as a protective membrane was studied in pH 7.4 PBS containing 0.5 mM ATCl. When the amount of NF (0.10 %) changed from 2 to 5 μl, the amperometric response gradually decreased and the RSD also gradually decreased. To ensure the sensitivity and stability of the AChE biosensor, 3 μl NF was chosen as the best compromise between the amperometric response and the RSD.

Effect of pH on the amperometric response of the NF/AChE–CS/SNS–NF/GCE biosensor

The bioactivity of the immobilized AChE depended on the pH of the ATCl solution. Figure 5 shows the relationship between the amperometric response of the biosensor and the pH of the ATCl solution; the standard deviation is 0.397 (n=5). The amperometric response increased with increasing pH and reached a maximum at pH 7.4. Further increase of the pH of the ATCl solution led to a gradual decrease of the amperometric response in the pH range from 6.8 to 8.0. Obviously, the maximum amperometric response was obtained at pH 7.4. This result indicates that pH 7.4 is the optimum pH for catalytic behavior of the NF/AChE–CS/SNS–NF/GCE biosensor.

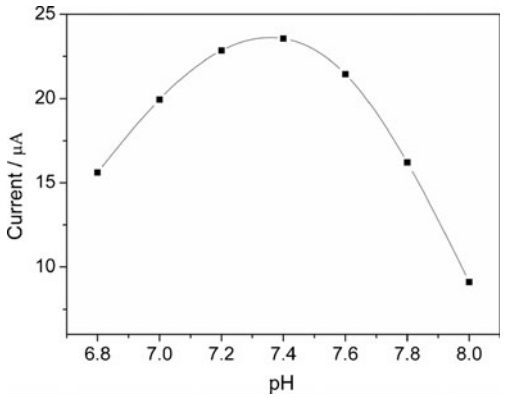

Fig. 5 Effect of pH on the amperometric response of the biosensor

Calibration plot of ATCl

The response of the NF/AChE-CS/SNS–NF/GCE biosensor to ATCl was explored in CV measurements. Figure 6 shows the amperometric response traces recorded with the NF/AChE–CS/SNS–NF/GCE polarized at 0.65 V in pH 7.4 PBS, to which was added an ATCl stock solution. With increasing ATCl concentration, the amperometric response of the AChE biosensor increased. The amperometric response of the biosensor is a linear function of ATCl concentration in two segments. One was from 0.2 to 20 μM, and the standard deviation on the intercept was 0.035 (n=5). The other was from 20 to 500 μM, and the standard deviation on the intercept was 0.553 (n=5). The detection limit was 0.1 μM. At higher ATCl concentrations, the shape of the response was indicative of a Michaelis–Menten process (Fig. 7). The apparent Michaelis–Menten constant (K_m^{app}) in the present studies was calculated to be 134 μM according to Eq. 1, and the standard deviation on the intercept was 0.002 (n=5). This value was lower than that for AChE immobilized on carbon nanotube–*N*,*N*-dimethylformamide composite film (0.66 mM) [19], for AChE immobilized on a polyethyleneimine-modified electrode (1.5 mM) [20], and for AChE immobilized on a gold nanoparticle–CS sol–gel composite modified electrode (0.35 mM) [21]. Owing to the excellent electron-transfer channels of SNS–NF, the immobilized AChE showed greater affinity for its substrate ATCl.

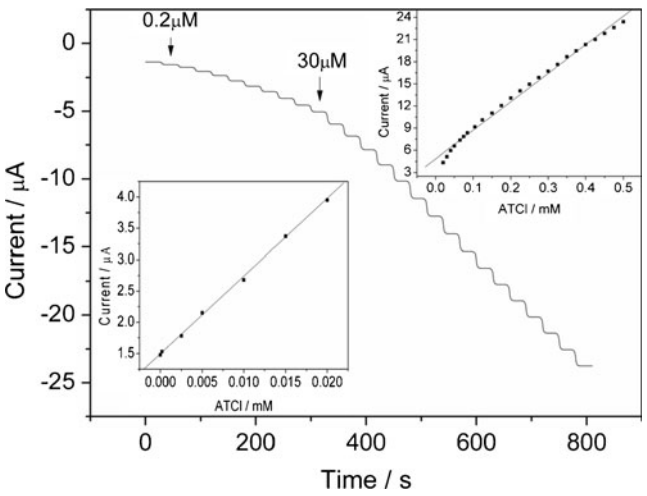

Fig. 6 Typical current–time plot for the biosensor on successive addition of stock ATCl to 0.1 M PBS, with stirring, at an applied potential of 0.65 V. The *insets* show the calibration curves for ATCl determination

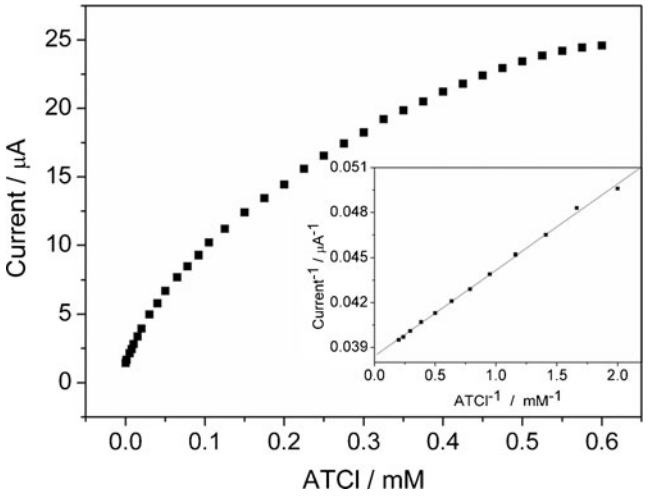

Fig. 7 Calibration plot for the ATCl biosensor. The *inset* shows the Lineweaver–Burk plot of $1/i_{ss}$ versus $1/C$

Effect of incubation time

It is recognized that pesticides have the same general structure and toxicological mode of action. In this work, methyl parathion was used as a model pesticide. The activity of AChE was influenced by the time for which AChE was incubated with methyl parathion. The inhibition level of AChE increased with increasing incubation time (Fig. 8). The standard deviation on the intercept was 0.9623 (n=5). Considering the whole analytical time and sensitivity of the amperometric measurements, an exposure time of 6 min was chosen as the best compromise between the signal and exposure time.

Detection of the pesticides

Methyl parathion bound to the active site of AChE to form a phosphorylated adduct when the biosensor was incubated in 0.1 M PBS containing methyl parathion. This inhibition led to a decrease of the activity and biological functions of

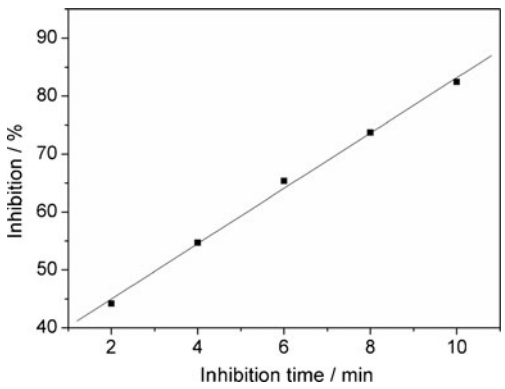

Fig. 8 Inhibition curves for different exposure times in 10^{-10}M methyl parathion

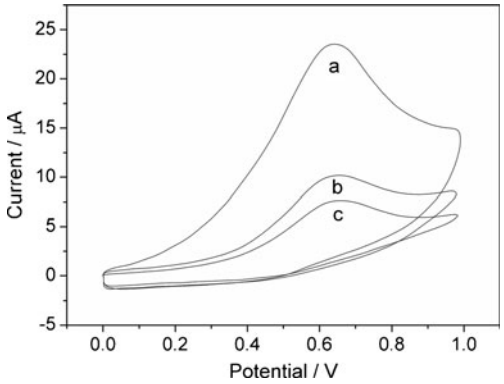

Fig. 9 Cyclic voltammograms of the NF/AChE–CS/SNS–NF/GCE in 0.1 M PBS containing 0.5 mM ATCl after incubation for 6 min with no (**a**), 10^{-11}M (**b**), and 10^{-9}M (**c**) methyl parathion

AChE. Therefore, detecting the amperometric response from thiocholine on the biosensor was a simple and effective way of biomonitoring pesticide exposure. As shown in Fig. 9, after incubation of the NF/AChE–CS/SNS–NF/GCE with 10^{-11}M methyl parathion for 6 min, the amperometric response (Fig. 9, curve b) decreased compared with that for the intact AChE (Fig. 9, curve a). After incubation of the NF/AChE–CS/SNS–NF/GCE with 10^{-9}M methyl parathion for 6 min, the amperometric response (Fig. 9, curve c) greatly decreased compared with that for the intact AChE (Fig. 9, curve a). Inhibition effects were investigated by measuring the response of the biosensor to 0.5 mM ATCl after inhibition by different concentrations of methyl parathion, chlorpyrifos, and carbofuran, respectively. The calibration plots of inhibition percentage versus pesticide concentration are shown in Fig. 10. Linear relationships between the inhibition percentage and the concentration of pesticides were obtained and are shown in Table S1. In Table 1, the

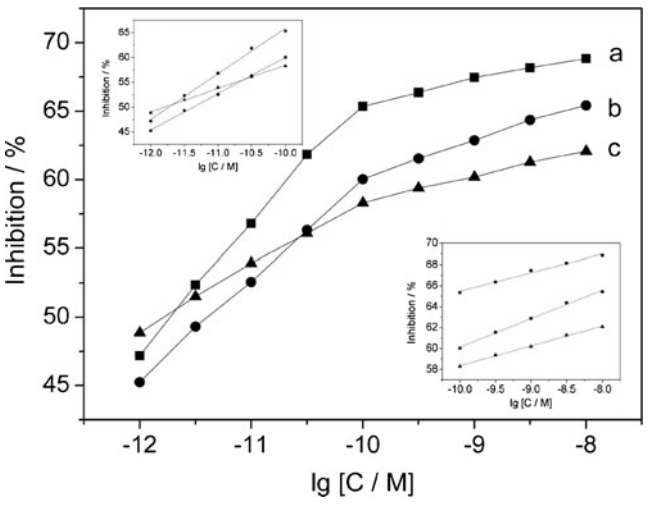

Fig. 10 Inhibition curve of the NF/AChE–CS/SNS–NF/GCE biosensor for determination of methyl parathion (**a**), chlorpyrifos (**b**), and carbofuran (**c**)

Table 1 Comparison of the response of the biosensor for detection of pesticides with other biosensors based on acetylcholinesterase (*AChE*)

Sample	Electrode	Liner range (M)	Detection limit (M)	References
Methyl parathion	AChE–LDHs/GCE	1.9×10^{-8}–1.1×10^{-6}; 1.1×10^{-6}–1.5×10^{-5}	2.3×10^{-9}	[23]
	AChE–SF/MWNTs/GCE	3.5×10^{-6}–2.0×10^{-3}	5.0×10^{-7}	[24]
	NF/AChE–CS/SNS–NF/GCE	10^{-12}–10^{-10}; 10^{-10}–10^{-8}	5.0×10^{-13}	This work
Chlorpyrifos	AChE/CPBA/GR–AuNPs/GCE	1.4×10^{-9}–2.9×10^{-8}; 2.9×10^{-8}–2.9×10^{-7}	2.9×10^{-10}	[25]
	NF/AChE–CS/SNS–NF/GCE	10^{-12}–10^{-10}; 10^{-10}–10^{-8}	5.0×10^{-13}	This work
Carbofuran	AChE/PAMAM–Au/CNTs/GCE	4.5×10^{-9}–9.0×10^{-8}	4.0×10^{-9}	[26]
	AChE–TCNQ/SPE	9.0×10^{-10}–7.5×10^{-7}	9.0×10^{-10}	[27]
	NF/AChE–CS/SNS–NF/GCE	10^{-12}–10^{-10}; 10^{-10}–10^{-8}	5.0×10^{-13}	This work

LDHs layered double hydroxides, *GCE* glassy carbon electrode, *SF* silk fibroin, *MWNTs* multiwalled carbon nanotubes, *NF* Nafion, *CS* chitosan, *SNS* SiO_2 nanosheets, *CPBA* 3-carboxyphenylboronic acid, *GR* graphene, *AuNPs* gold nanoparticles, *PAMAM* polyamidoamine, *CNTs* carbon nanotubes, *TCNQ* 7,7,8,8-tetracyanoquinodimethane, *SPE* screen-printed electrode

performances of the biosensor are compared with those of other AChE biosensors reported in the literature.

Regeneration of AChE

Regeneration is one of the key issues in the development of biosensors based on enzyme inhibition. Different approaches, such as simple rinsing with buffer, incubation with PAM regeneration reagents, and high concentration of ATCl, have been applied [22]. The amperometric response of the biosensor before and after exposure of AChE to methyl parathion was tested.

First, the initial amperometric response of the biosensor was 23.55 μA in 0.1 M PBS containing 0.5 mM ATCl. After incubation for 6 min in 0.1 M PBS containing 10^{-11} M methyl parathion, the amperometric response of the biosensor was 10.18 μA in 0.1 M PBS containing 0.5 mM ATCl. After rinsing with 0.1 M PBS and incubation in 0.1 M PBS containing 0.1 mM PAM and 0.1 M PBS containing 10 mM ATCl for 2 min, respectively, the amperometric response of the biosensor recovered to 23.18 μA in 0.1 M PBS including 0.5 mM ATCl. After incubation for 6 min in 0.1 M PBS containing 10^{-9} M methyl parathion, the amperometric response of the biosensor was 7.66 μA in 0.1 M PBS containing 0.5 mM ATCl. After the second regeneration step, the amperometric response of the biosensor recovered to 22.86 μA. This result shows that the activity of AChE recovered after the regeneration. So successive rinsing and incubation in 0.1 mM PAM and 10 mM ATCl, respectively, were used to regenerate the biosensor.

Table 2 Possible interferences tested with the biosensor

Interfering species[a]	Concentration (mM)	Amperometric response (μA)
Control[b]	0.5	23.55
Glucose	0.5	23.19
Citric acid	0.5	23.52
Oxalic acid	0.5	23.72
p-Nitrophenol	0.5	13.96

[a] Interfering species exist in 0.1 M phosphate-buffered saline (PBS) containing 0.5 mM acetylthiocholine chloride (ATCl)

[b] This was 0.1 M PBS containing 0.5 mM ATCl

Interference study

The interfering signal due to the commonest electroactive species was studied. The signal for 0.5 mM ATCl was compared with the signal obtained in the presence of the interfering species. The test result showed no noticeable changes in amperometric response were detected in the presence of glucose (0.5 mM), citric acid (0.5 mM), and oxalic acid (0.5 mM), respectively, at the operating potential used in this system. However, the amperometric response decreased obviously in the presence of 0.5 mM *p*-nitrophenol. The results of the interference study are shown in Table 2. Interferences from other organophosphate and carbamate pesticides were also studied. Mixtures of species of equal concentration of methyl parathion and chlorpyrifos, methyl parathion and carbofuran, and chlorpyrifos and carbofuran were determined. The inhibitions of the three mixtures of pesticides decreased obviously. The results showed methyl parathion, chlorpyrifos, and carbofuran interfere with each other.

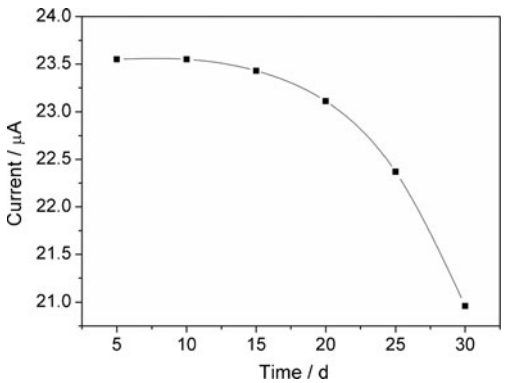

Fig. 11 Variation of amperometric response of the biosensor with time

Precision of measurements and stability of the biosensor

The intra-assay precision of the biosensor was evaluated by assaying one enzyme electrode for six replicate determinations in 0.5 mM ATCl after it had been immersed in 1.0×10^{-10}M methyl parathion for 6 min. Similarly, the inter-assay precision, or fabrication reproducibility, was estimated at six different electrodes. The RSDs of intra-assay and inter-assay precisions were 4.4 % and 6.2 %, respectively, indicating acceptable reproducibility. When the enzyme electrode was not in use, it was stored at 4 °C in a dry condition. No obvious decrease in the amperometric response of ATCl was observed in the first 10 days of storage. After a 30-day storage period, the sensor retained 89 % of its initial amperometric response, indicating acceptable stability of the biosensor (Fig. 11).

Real analytical samples

This method was applied to the determination of methyl parathion in apple and cabbage. A standard addition method was adopted to estimate the accuracy. The determination results are shown in Table S2. No amperometric response corresponding to methyl parathion was observed when the samples were analyzed, meaning that their concentrations were below the detection limits. The recoveries of the standards added ranged from 94.0 % to 103.0 %, indicating that the method had some reliability.

Conclusion

In this work, SNS were successfully prepared and characterized. Combining the advantageous characteristics of SNS and NF, an SNS–NF nanocomposite was prepared. The SNS–NF nanocomposite had excellent conductivity, catalytic activity, and biocompatibility and provided an extremely hydrophilic surface that was favorable for AChE adhesion, biological activity maintenance, and conductivity between AChE and the modified electrode. CS was used as a cross-linker to immobilize AChE on the SNS–NF/GCE, and NF was used as a protective membrane for the AChE biosensor to improve its stability. An NF/AChE–CS/SNS–NF/GCE biosensor was fabricated and exhibited many advantages, such as low applied potential, fast response, high sensitivity, acceptable stability, reproducibility, simple fabrication, and low cost. The concept can be extended to assemble other biological molecules, such as antibodies, antigens, and DNA, on the SNS–NF surface for wide bioassay applications.

References

1. Yu Q, Li Y, Ma AZ, Liu WF, Wang HL, Zhuang GQ (2011) Anal Bioanal Chem 401:2891–2898
2. Schulze H, Schmid RD, Bachmann TT (2002) Anal Bioanal Chem 372:268–272
3. McGrath TF, Elliott CT, Fodey TL (2012) Anal Bioanal Chem 403:75–92
4. Yang CY, Zhang ZJ, Shi ZL, Xue P, Chang PP, Yan RF (2010) Anal Bioanal Chem 397:2997–3003
5. Rawal R, Chawla S, Dahiya T, Pundir CS (2011) Anal Bioanal Chem 401:2599–2608
6. Kresge CT, Leonowicz ME, Roth WJ, Vartuli JC, Beck JS (1992) Nature 359(6397):710–712
7. Zhang XY, Liu DX, Xu DD (2012) Science 29:1684–1687
8. Rosenholm JM, Meinander A, Peuhu E, Niemi R, Eriksson JE, Sahlgren C, Linden M (2009) ACS Nano 3:197–206
9. Trewyn B-G, Slowing I-I, Giri S, Chen H-T, Lin V-S-Y (2007) Acc Chem Res 40:846–853
10. Abdullah J, Ahmad M, Heng LY, Karuppiah N, Sidek H (2006) Anal Bioanal Chem 386:1285–1292
11. Zhang FF, Wan Q, Li CX (2004) Anal Bioanal Chem 380:637–642
12. Hoyer B, Florence TM, Batley GE (1987) Anal Chem 59:1608–1614
13. Hu ZM, Seliskar CJ, Heineman WR (1998) Anal Chim Acta 369:93–101
14. Kumaravel A, Chandrasekaran M (2010) J Electroanal Chem 638:231–235
15. Jing L, Guo SJ, Zhai YM (2009) Electrochem Commun 11:1085–1088
16. Fan Y, Liu J-H, Lu H-T (2011) Colloids Surf B Biointerfaces 85:289–292
17. Li MG, Xu SD, Tang M (2011) Electrochim Acta 56:1144–1149
18. Wang YY, Wang XS, Wu BY, Zhao ZX, Yin F, Li S, Qin X (2008) Sens Actuators B 130:809–815
19. Joshi KA, Tang J, Haddon R, Wang J, Chen W, Mulchandani A (2005) Electroanalysis 17:54–58
20. Vakurov A, Simpson CE, Daly CL, Gibson TD, Millner PA (2004) Biosens Bioelectron 20:1118–1125
21. Du D, Chen SZ, Cai J, Song DD (2007) J Electroanal Chem 611:60–66
22. Liu GD, Lin YH (2006) Anal Chem 78:835–843
23. Gong JM, Guan ZQ, Song DD (2013) Biosens Bioelectron 39:320–323
24. Xue R, Kang TF, Lu LP, Cheng SY (2012) Appl Surf Sci 258:6040–6045
25. Liu T, Su HC, Qu XJ (2011) Sens Actuators B 160:1255–1261
26. Qu Y, Sun Q, Xiao F, Shi G, Jin L (2010) Bioelectrochemistry 77:139–144
27. Nunes GS, Jeanty G, Marty JL (2004) Anal Chim Acta 523:107–115